



# Retrocardiac Opacities Detected on Chest Radiographs and their Imaging Workup: A Pictorial Review

Divya Saikumar<sup>1</sup> K. Ramachandran<sup>1</sup> P.K.M. Zunimol<sup>1</sup>

<sup>1</sup>Department of Radiology, Kerala Institute of Medical Sciences, Thiruvananthapuram, Kerala, India

Indographics 2023;2:28–38.

Address for correspondence Dr. Divya Saikumar, 12H, Sowparnika Promenade Square Apartments, Poonthi Road, Anayara, Thiruvananthapuram, Kerala 695033, India (e-mail: divyaamrita1997@gmail.com).

## Abstract

The retrocardiac space is a tricky area in the chest radiograph, where abnormal densities are frequently missed out. Lesions in this area produce late pressure symptoms compared with those in the upper mediastinum. Early detection and proper evaluation of retrocardiac opacities can help the radiologist to establish the diagnosis before clinical signs and symptoms become apparent. We present a case series of 10 patients with incidentally detected retrocardiac opacities in the frontal chest radiograph, which were further evaluated with other imaging modalities such as lateral chest radiograph, computed tomography (CT) or magnetic resonance imaging (MRI) to establish the diagnosis. The final diagnosis included congenital conditions like esophageal duplication cyst and bronchogenic cyst; inflammatory conditions like spondylodiscitis, lung abscess, and lobar pneumonia; vascular conditions like aortic aneurysm; diaphragmatic pathologies like hiatus hernia; and rare tumors like cardiac papillary fibroelastoma, pulmonary neuroendocrine tumor, and ganglioneuroma. Cardinal signs that aid in the diagnosis of retrocardiac opacities are also discussed.

## Keywords

- ▶ retrocardiac opacities
- ▶ retrocardiac space
- ▶ chest radiograph
- ▶ retrocardiac sail sign
- ▶ cardiac shadow

## Introduction

The retrocardiac space is defined as the space between the posterior border of the heart and the vertebral column in the lateral chest radiograph (▶ **Figs. 1–2**). This was first described by Austrian radiologist Dr. Guido Holzkecht (▶ **Fig. 3**). This is a tricky space in the chest radiograph where abnormal densities can be frequently missed out. The space occupying lesions in the upper half of the mediastinum often produce pressure symptoms early, thus enabling prompt detection and management of these lesions by the clinician. However, the retrocardiac space is wide and lesions must reach considerable size before they lead to clinical signs and symptoms. Early detection and prompt evaluation of abnormal densities in the

retrocardiac region may help the radiologist to establish the diagnosis before the clinical signs and symptoms become apparent, thus enabling prompt clinical management before it becomes too late. In this article, we review how the imaging workup of 10 incidentally detected retrocardiac opacities on the chest radiograph led to 10 different diagnosis and aided in prompt clinical management. An algorithmic approach to retrocardiac opacities and their differential diagnosis have also been discussed in this article.

## The Cardiac Silhouette

The pericardium and the heart cast a triangular shadow on a posteroanterior (PA) chest radiograph. The right border of

DOI <https://doi.org/10.1055/s-0043-1771239>.  
ISSN 2583-8229.

© 2023, Indographics. All rights reserved.

This is an open access article published by Thieme under the terms of the Creative Commons Attribution-NonDerivative-NonCommercial-License, permitting copying and reproduction so long as the original work is given appropriate credit. Contents may not be used for commercial purposes, or adapted, remixed, transformed or built upon. (<https://creativecommons.org/licenses/by-nc-nd/4.0/>)

Thieme Medical and Scientific Publishers Pvt. Ltd., A-12, 2nd Floor, Sector 2, Noida-201301 UP, India

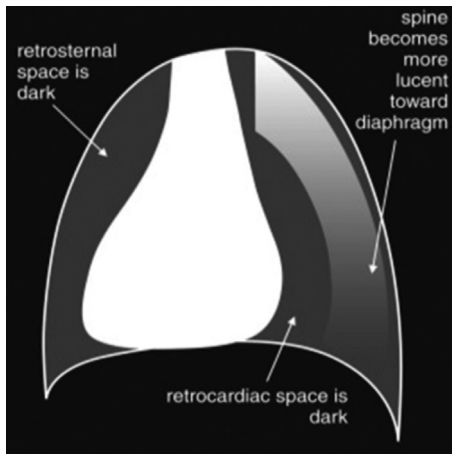


**Fig. 1** Illustrative diagram of the retrocardiac space.



**Fig. 3** Dr. Guido Holzknrecht, Austrian radiologist. (This image is provided courtesy of Wikipedia.)

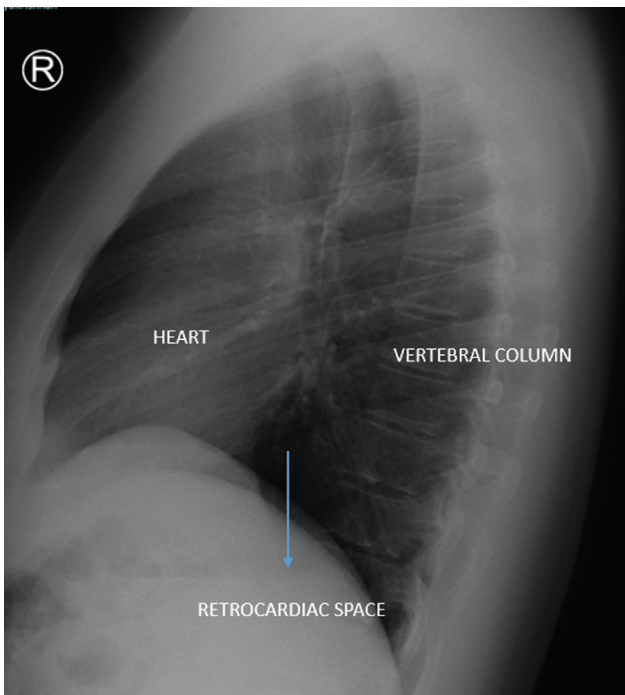


**Fig. 2** The retrocardiac space on a lateral chest radiograph.

the heart on a PA chest radiograph is formed by the superior vena cava superiorly, and the right atrium and the inferior vena cava at its lower margin. The left border of the heart is formed by the aortic knob for the arch of aorta, main pulmonary artery, left atrium, and left ventricle from above downward (→Fig. 4). Normally, the cardiac shadow is not separately visualized within the larger silhouette of the pericardium as a central nuclear shadow. Other normal shadows visualized within the cardiac silhouette are the following:

- *Pulmonary markings:* They extend obliquely from the hila toward the diaphragm. They are often superimposed over the left peripheral portion of the cardiac shadow and a few markings are seen on the right.

- *Epicardial pad of fat:* They are often visualized as a triangular area of decreased density adjacent to the apex of the heart.
- *Descending thoracic aorta:* The para-aortic line formed by the descending thoracic aorta is visualized toward the left of the spine superimposed over the cardiac shadow.
- Paraspinal shadows.

The presence of other shadows within the cardiac silhouette needs to be investigated in detail. Broadly, six patterns of retrocardiac opacities have been described (→Figs. 5 and 6, →Table 1).<sup>1</sup>

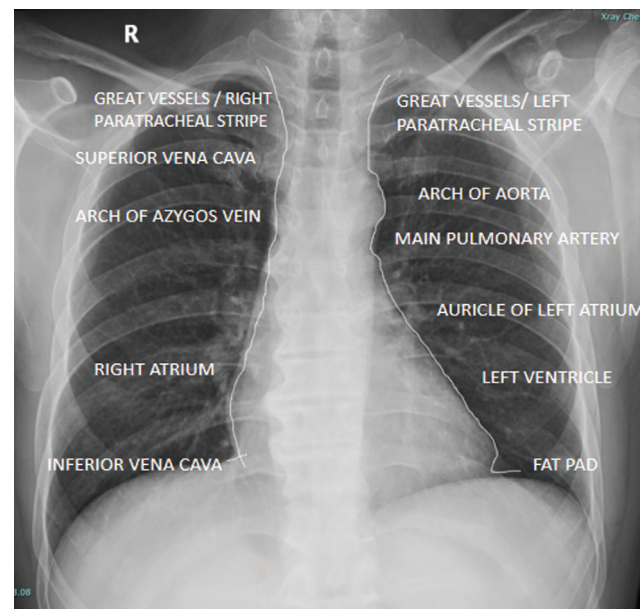


**Fig. 4** The cardiac silhouette.

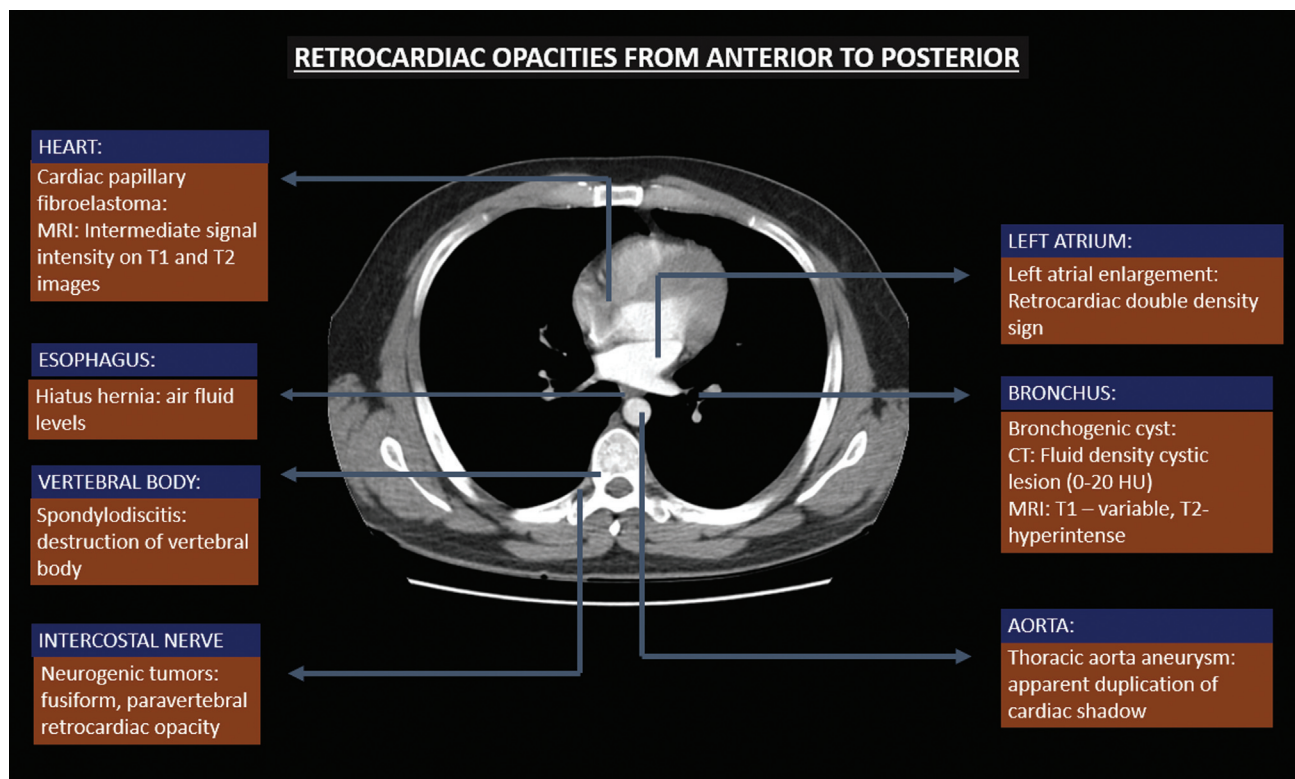


**Fig. 5** A cross-sectional diagram illustrating retrocardiac opacities from anterior to posterior. CT, computed tomography; MRI, magnetic resonance imaging.

**Apparent Duplication of the Cardiac Shadow**

A cardiac shadow cannot be directly seen within the larger silhouette of a pericardial effusion. Apparent duplication of

the cardiac shadow is thus due to other conditions like diaphragmatic hernias, thoracic stomach with congenitally short esophagus, mega esophagus, and aortic aneurysm.<sup>1</sup>

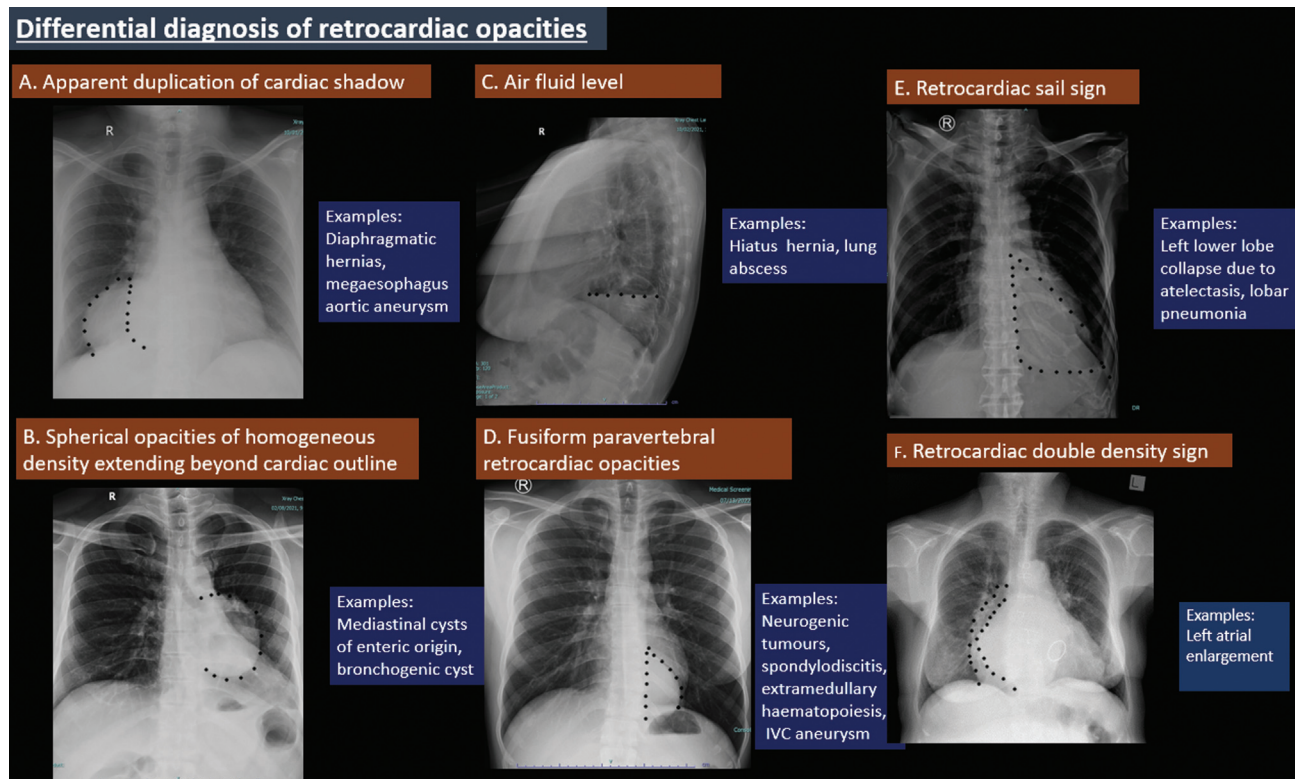


**Fig. 6** (A–F) Differential diagnosis of retrocardiac opacities.

**Table 1** Age group wise categorization of retrocardiac opacities

Age group	Retrocardiac opacities
Pediatric (0–20 y)	Bronchogenic cyst, enteric duplication cyst, and extramedullary hematopoiesis
Middle aged (20–60 y)	Hiatus hernia, esophageal varices, spondylodiscitis, extramedullary hematopoiesis, inferior vena cava (IVC) aneurysm, left atrial enlargement, and neurogenic tumors
Elderly (>60 y)	Atherosclerotic aortic aneurysm

The presence of multiple convex lines outlining the retrocardiac opacity is an important diagnostic sign indicating that the stomach is in the retrocardiac region (►Fig. 7). This sign was first described by Holmes.<sup>2</sup> Aneurysm of the descending thoracic aorta is often visualized through the left half of the cardiac shadow as a fusiform or globular retrocardiac opacity causing apparent duplication of the cardiac shadow (►Fig. 8).<sup>3</sup> The importance of studying the variations in density of the cardiac shadow in the early diagnosis of lobar pneumonia of the lower lobes, localized bronchiectasis, lung abscess, and mediastinal pleural effusion was pointed out by Rigler.<sup>4</sup>

**Spherical Opacities of Homogeneous Density Extending Beyond the Cardiac Outline**

Mediastinal cysts of enteric origin like esophageal duplication cyst and bronchogenic cysts often appear as spherical retrocardiac opacities extending beyond the cardiac outline. Mediastinal cysts of enteric origin usually arise in the posterior mediastinum in the middle third, but their occurrence in the retrocardiac region has been reported by Ladd and Scott.<sup>5</sup> Bronchogenic cysts result from abnormal ventral budding or branching of the tracheobronchial tree during embryologic development. They may occur in any part of the mediastinum, but most are near the tracheal carina in the middle or posterior mediastinum. Less often, they may occur

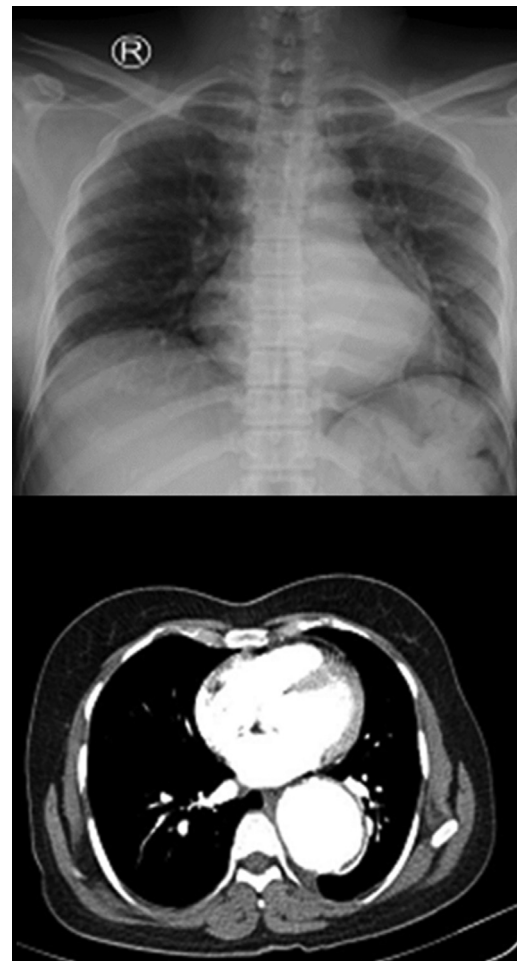


**Fig. 8** A 48-year-old woman presented to the orthopaedics outpatient department (OPD) with complaints of backache for 3 months. Incidental detection of a fusiform retrocardiac opacity in the posteroanterior (PA) chest radiograph. Further evaluation with computed tomography (CT) aortic angiogram revealed an aneurysmal dilatation of the descending thoracic aorta. Final diagnosis: Descending thoracic aorta aneurysm.

within the lung parenchyma, pleura, or diaphragm. On conventional chest radiographs, a bronchogenic cyst usually appears as a well-defined solitary mass with a homogeneous opacity just inferior to the carina and often protruding

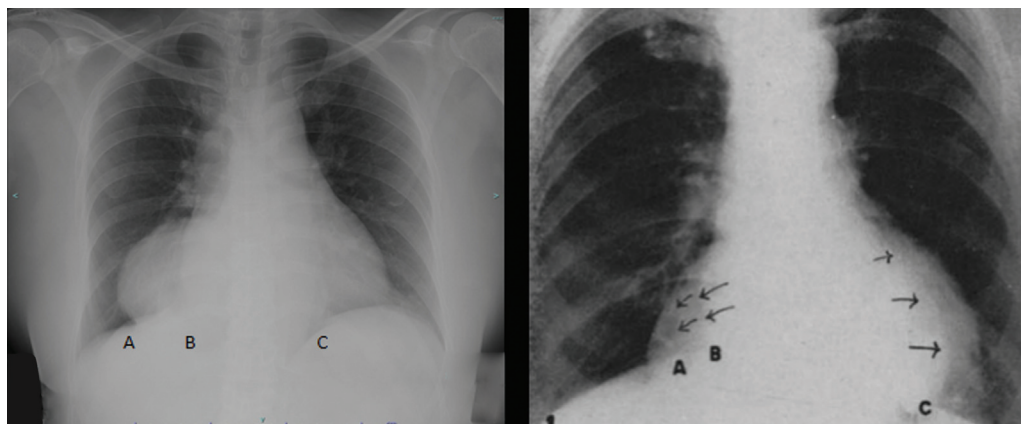


**Fig. 7** Duplication of the cardiac shadow produced by the stomach in the retrocardiac region. Note the convex lines A, B, and C within the cardiac shadow.

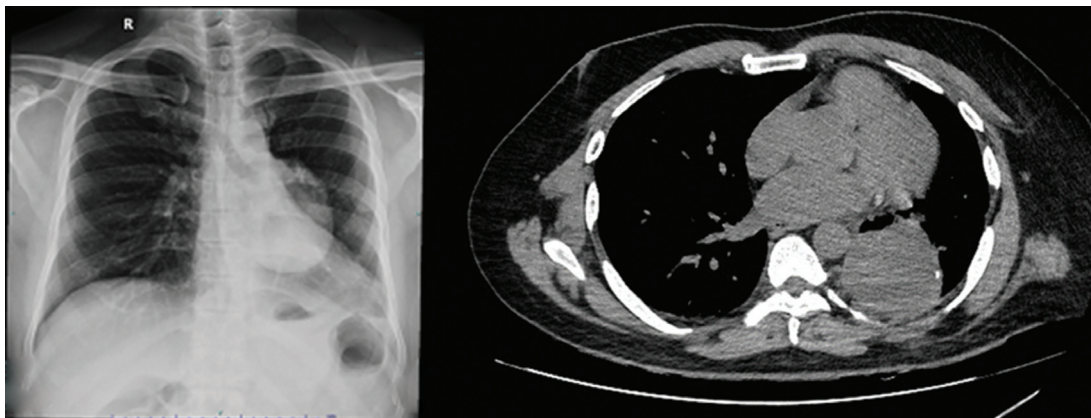


**Fig. 9** A 53-year-old gentleman presented to the emergency room with a history of road traffic accident. A posteroanterior (PA) chest radiograph revealed a well-defined, homogeneous retrocardiac opacity in the left hilar region. Plain computed tomography (CT) of the chest revealed a well-defined, left paravertebral soft-tissue density lesion suggestive of a posterior mediastinal space occupying lesion compressing the left lower lobe bronchus. No communication with the bronchus is noted. No wall calcifications are noted. Final diagnosis: Bronchogenic cyst.

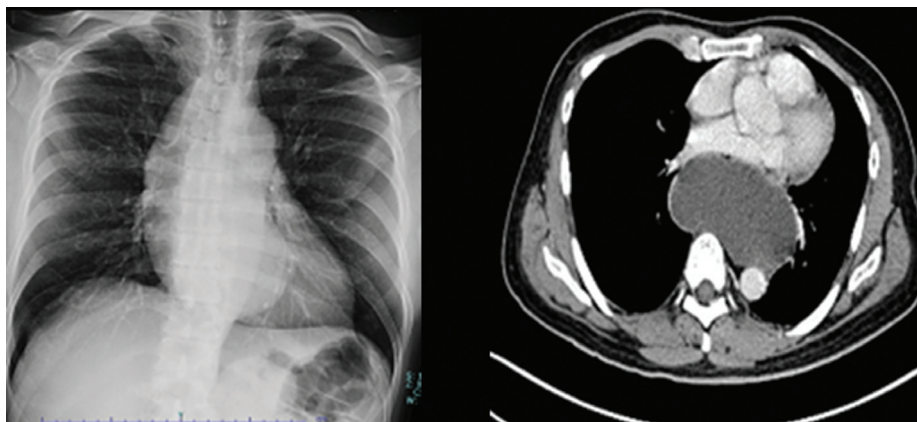


**Fig. 10** A 48-year-old gentleman presented to the gastroenterology outpatient department (OPD) with complains of bleeding per rectum and weight loss for 6 months. There is incidental detection of a fusiform retrocardiac opacity in the left paravertebral region. Contrast-enhanced computed tomography (CT) of the chest, abdomen, and pelvis revealed a large, well-defined, fluid-attenuating cystic lesion along the thoracic esophagus extending from T3 to T10/T11 vertebral levels causing anterior displacement and luminal narrowing of the esophagus. Final diagnosis: Esophageal duplication cyst.

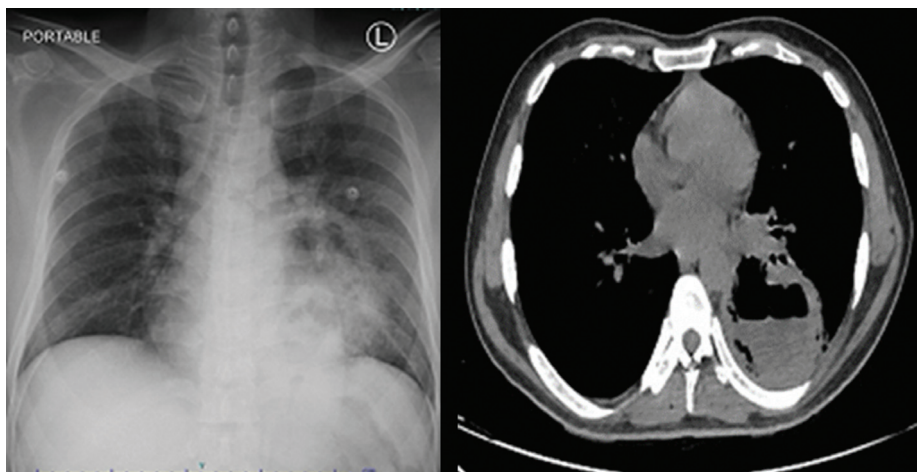


**Fig. 11** A 44-year-old gentleman presented to the emergency room with complains of acute abdominal pain radiating to the back. Amylase and lipase were elevated. Posteroanterior (PA) chest radiograph revealed an irregular, nonhomogeneous retrocardiac opacity in the left paravertebral region. Plain computed tomography (CT) of the chest, abdomen, and pelvis revealed a soft-tissue density lesion with air fluid levels and surrounding air bronchograms noted in the superior basal, anteromedial basal, and posterior basal segments of left lower lobe. Final diagnosis: Lung abscess secondary to pancreatic pseudocyst rupture.

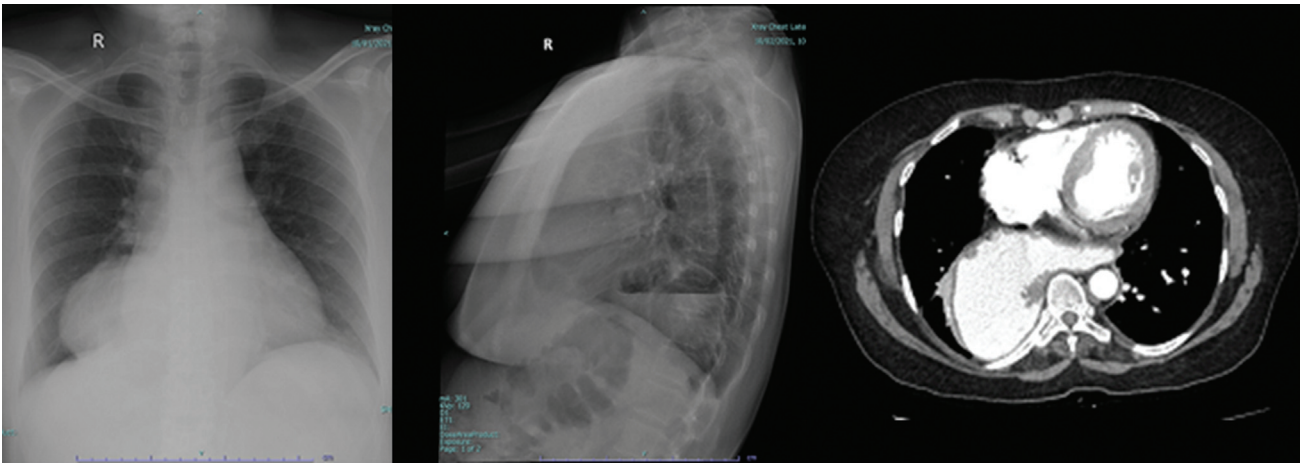


**Fig. 12** A 9-year-old girl presented to the gastroenterology outpatient department (OPD) with complaints of bloating and flatulence for 2 months. There was incidental detection of a well-defined, oval, retrocardiac opacity in the right lower zone medially in the posteroanterior (PA) chest radiograph. Lateral chest radiograph confirmed the presence of an air fluid level within the lesion. Further evaluation with contrast-enhanced computed tomography (CT) of the chest revealed a widened esophageal hiatus of the diaphragm with herniation of the fundus and part of the body of the stomach into the lower right hemithorax. Final diagnosis: Right-sided hiatus hernia.

slightly toward the right hilar shadow. On computed tomography (CT) scans, a bronchogenic cyst appears as a single, smooth, elliptic, or round mass with an imperceptible wall and uniform attenuation (►Fig. 9).<sup>6</sup> Esophageal duplication cysts are developmental in origin and are classified as foregut cysts that are either bronchogenic or neurenteric. Appearance at CT or magnetic resonance (MR) imaging is identical to that of bronchogenic cysts except that the wall of the lesion may be thicker and in more close contact with the esophagus (►Fig. 10).<sup>7</sup> Sympathicoblastoma occurring in children may produce a round or fusiform retrocardiac opacity that may extend even beyond the cardiac outline. Destruction of the pedicles and sclerosis of the body of the vertebra adjacent to the sympathicoblastoma is often observed.<sup>8</sup>

### Retrocardiac Air-Fluid Level

The presence of air fluid levels within retrocardiac opacities is seen in hiatus hernia and lung abscess (►Fig. 11). A single retrocardiac air-fluid level on a chest radiograph is usually noted in the presence of a sliding hiatal hernia. Up to 85% of such hernias are noted to be left-sided through the foramen of Bochdalek, whereas right-sided hernias through the foramen of Morgagni are far less common than the former (►Fig. 12).<sup>9</sup> Left-sided diaphragmatic hernias are more common, because the right pleuroperitoneal canal closes earlier and the liver protects the right diaphragm.<sup>10</sup> A differential retrocardiac fluid level (two air-fluid interfaces at different heights) is observed in intrathoracic gastric volvulus. The one in the retrocardiac mediastinum represents the dilated, herniated distal stomach and the one beneath the left hemidiaphragm represents an air-fluid level in the normally positioned fundus, which may be partially obstructed at the inlet to the twisted hernial segment.<sup>11</sup>

### Fusiform Paravertebral Retrocardiac Opacities

Tumors of neurogenic origin like ganglioneuromas, neurofibromas, schwannomas, and neuroblastomas frequently

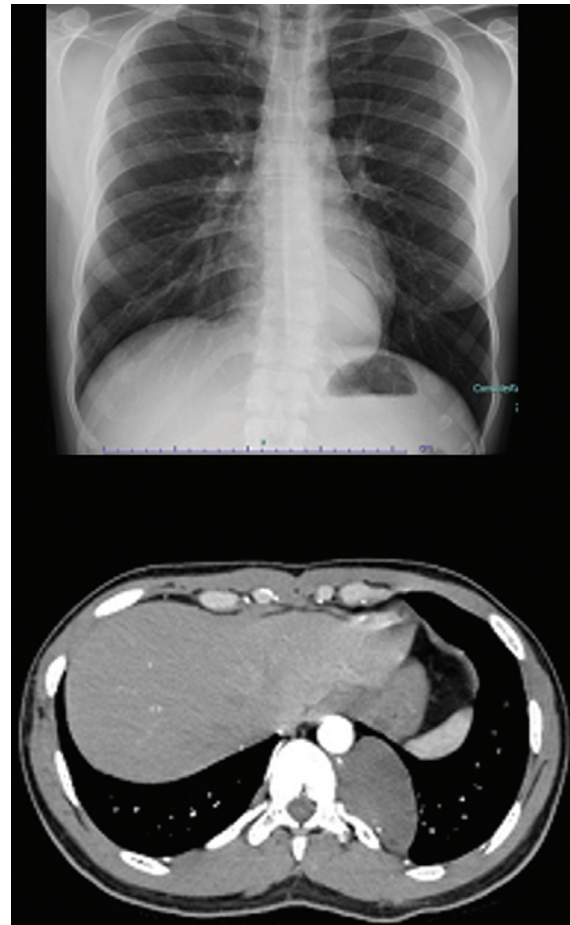


**Fig. 13** A 30-year-old gentleman came for a routine executive checkup. There was incidental detection of a left paravertebral retrocardiac opacity on the posteroanterior (PA) chest radiograph. Further evaluation with contrast-enhanced computed tomography (CT) revealed a well-defined, hypoenhancing, left paravertebral soft-tissue density lesion suggestive of posterior mediastinal mass at the T11-T12 level with neural foramina communication. Final diagnosis: Ganglioneuroma.

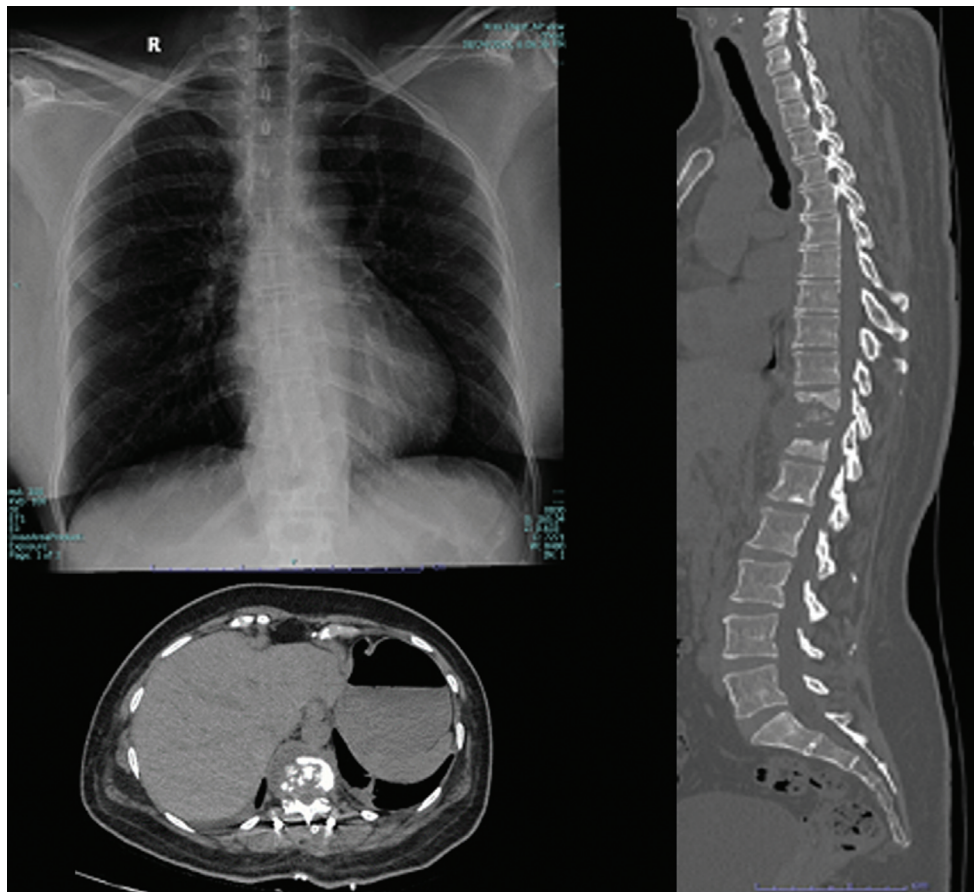


**Fig. 14** A 50-year-old woman presented to the orthopaedics outpatient department (OPD) with complains of low back ache for 3 months. Posteroanterior (PA) chest radiograph revealed a right paravertebral retrocardiac opacity at the level of the T11–T12 vertebrae with destruction of adjacent pedicles. Plain computed tomography (CT) of the chest revealed an irregular lytic destruction of the T11–T12 vertebral bodies with associated paravertebral soft-tissue component. Intervertebral disk involvement was also noted. Final diagnosis: spondylodiscitis (tuberculosis of the spine).

present as paravertebral retrocardiac opacities. They usually appear as single, sharply outlined, rounded or oval non-pulsating shadows on one side of the vertebral column (►Fig. 13).<sup>1</sup> Kent et al pointed out that the lobulated appearance of a neurogenic tumor is strongly suggestive of rapid growth and thus malignancy.<sup>12</sup> Naffziger et al emphasized the need of radiographic study of the intervertebral foramina, and interspinous and interlaminar spaces to detect areas of erosion produced by these tumors.<sup>13</sup>

Intrathoracic extramedullary hematopoiesis often presented as paravertebral retrocardiac opacities. They usually present as bilateral lobulated masses in the lower paravertebral regions. Destruction of adjacent ribs and vertebrae is not seen in extramedullary hematopoiesis.<sup>14</sup>

spondylodiscitis of the spine often present as fusiform paravertebral retrocardiac opacities with destruction of the adjacent vertebrae (►Fig. 14). In patients with chronic liver disease, portal hypertension with paraesophageal varices can present as paravertebral retrocardiac opacities.<sup>15–17</sup> An unusual case of an inferior vena cava aneurysm presenting as a retrocardiac paravertebral mass on the chest radiograph has been reported.<sup>18</sup>

### Retrocardiac Sail Sign

Retrocardiac sail sign represents the highly specific appearance of left lower lobe collapse on a frontal chest radiograph (►Fig. 15). The collapsed medially displaced left lower lobe is represented by a triangular area of increased density with sharp margins, superimposed over the heart shadow. It resembles the unfurled sail of a yacht. The heart contour remains preserved, while the contour of the left hemidiaphragm is at least partially effaced (►Fig. 16).

### Retrocardiac Double-Density Sign

The retrocardiac double-density sign is also known as the “double right heart border” sign. This sign is seen on frontal chest radiographs in the presence of left atrial enlargement and occurs when the right side of the left atrium extends behind the right cardiac shadow, indenting the adjacent lung and forming its own silhouette. (►Fig. 17).<sup>19</sup>

### Miscellaneous Masses Causing Retrocardiac Opacities

Two other incidentally retrocardiac opacities were detected in the chest radiograph. Further evaluation of these opacities led to the diagnosis of cardiac papillary fibroelastoma and

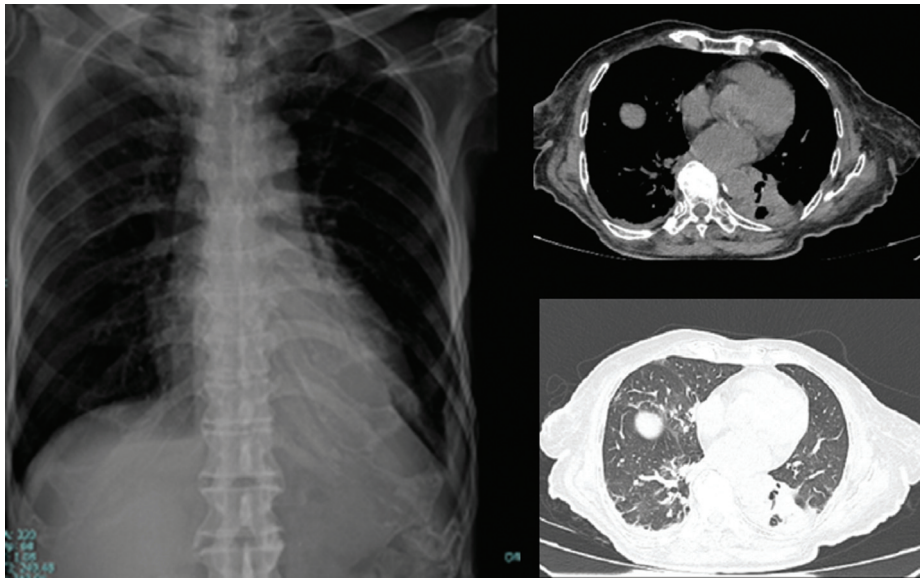


**Fig. 15** An 80-year-old gentleman presented to the emergency room with complaints of fever, cough, and breathlessness. Posteroanterior (PA) chest radiograph revealed a retrocardiac triangular opacity in the left lower zone with obliteration of the left dome of the diaphragm medially. Plain computed tomography (CT) of the chest revealed a subsegmental collapse consolidation with air bronchogram involving the superior and basal segments of the left lower lobe with associated partial volume loss. Final diagnosis: Left lower lobe pneumonia.

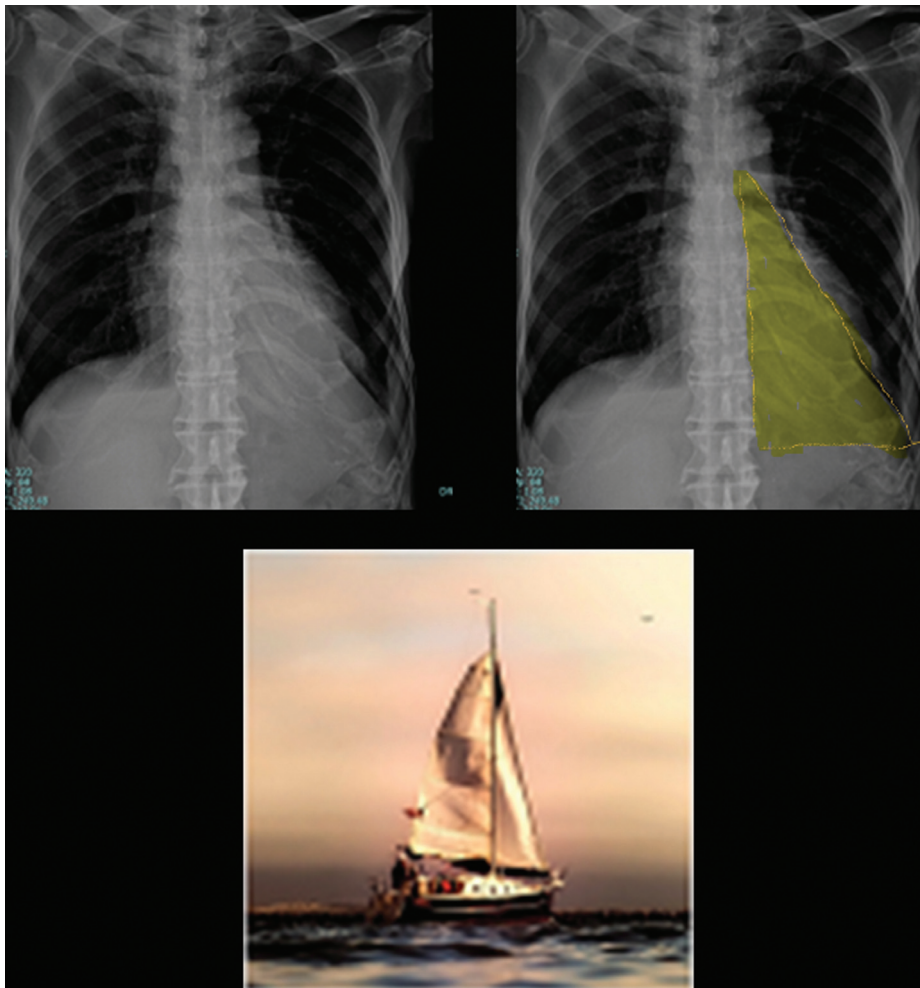


**Fig. 16** The retrocardiac sail sign.



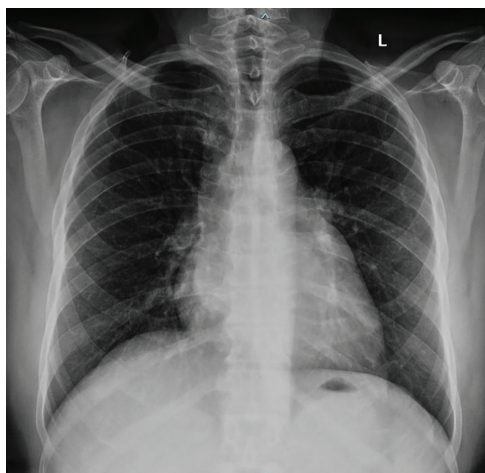


**Fig. 17** A 40-year-old gentleman who was a known case of rheumatic heart disease presented with complaints of dyspnea and palpitations since 1 week. Posteroanterior (PA) chest radiograph revealed a “retrocardiac double density shadow” sign due to enlarged left atrium.

pulmonary neuroendocrine tumor. They presented as well-defined, rounded retrocardiac opacities. Papillary fibroelastomas are one of the most common types of benign primary cardiac tumors. They are a potential cause of transient ischemic attacks, strokes, myocardial infarction, and sudden death (**►Fig. 18**).<sup>20</sup>

Carcinoid tumors are neuroendocrine neoplasms originating from enterochromaffin cells. Pulmonary neuroendocrine neoplasms appear as relatively well-defined rounded hilar/perihilar masses often associated with distal parenchymal diseases such as consolidations or atelectasis on chest radiographs. Endobronchial pulmonary neuroendocrine tumors often appear as triangular retrocardiac opacities due to atelectasis of the distal lung segments (**►Fig. 19**).<sup>21</sup>

Factors affecting radiographic image quality like contrast, spatial resolution, noise, and artifacts can affect the detection of retrocardiac opacities in the chest radiograph. It is important to obtain radiographic images with better contrast adjustment, spatial resolution, reduced noise, and

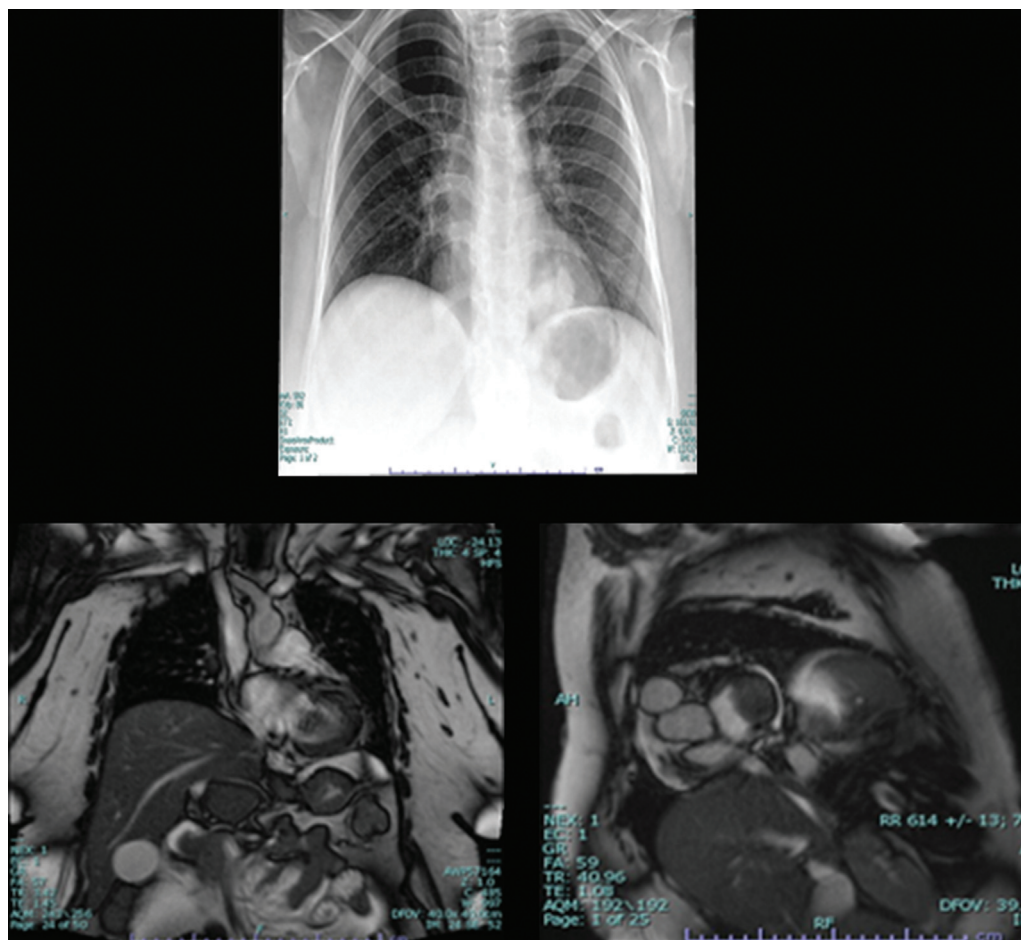


**Fig. 18** A 59-year-old woman presented to the emergency room with complaints of seizures. There was incidental detection of a well-defined retrocardiac opacity in the left lower zone on the posteroanterior (PA) chest radiograph. Routine echocardiogram done for the patient revealed a mitral valve mass. Further evaluation with cardiac magnetic resonance imaging (MRI) revealed a well-defined, mildly enhancing oval mass lesion at the ventricular aspect of the posterior leaflet of the mitral valve, possibly adherent to the chordae tendineae of the posterior papillary muscle and lateral basal left ventricular myocardium. Final diagnosis on histopathology: Cardiac papillary fibroelastoma.

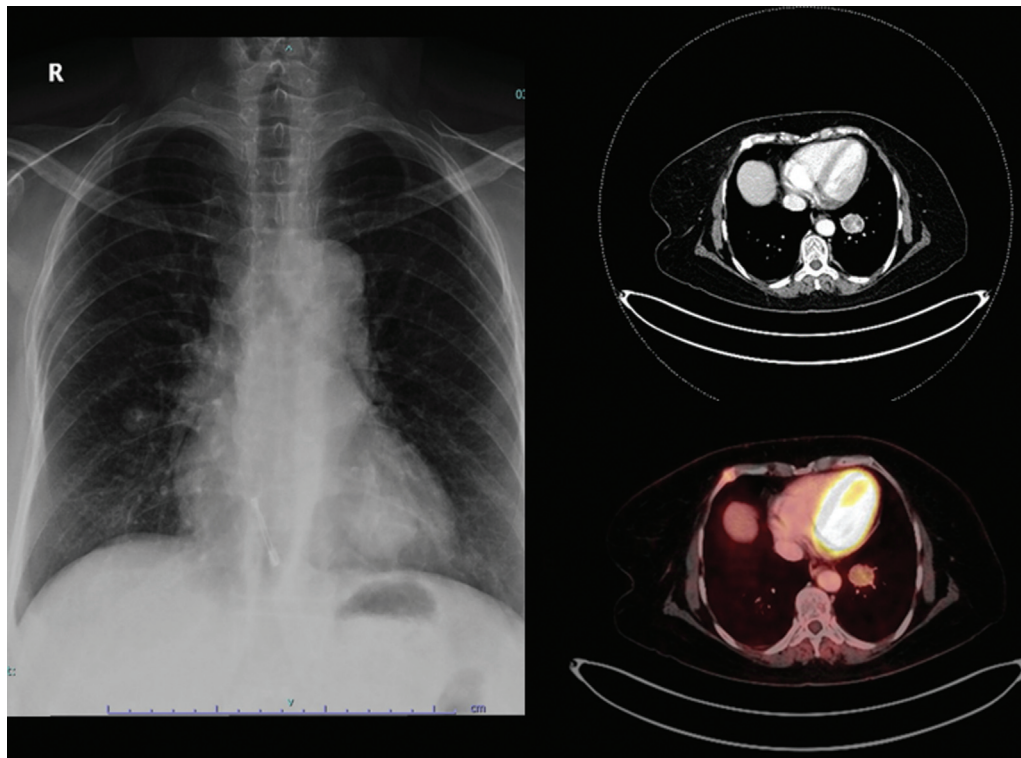


**Fig. 19** A 62-year-old lady presented to the emergency room with a history of slip and fall. There was incidental detection of a retrocardiac rounded opacity in the left lower zone and another small, rounded opacity in the right mid-zone on posteroanterior (PA) chest radiograph. Contrast-enhanced computed tomography (CT) of the chest revealed a nodule with heterogeneous enhancement in the medial basal segment of the left lower lobe with multiple small nodules in the peribronchovascular region, likely metastasis. Further evaluation with positron emission tomography (PET) CT revealed fluorodeoxyglucose (FDG) avid soft-tissue density lesions in the medial basal segment of the left lower lobe, anterior segment of the right upper lobe, and lateral segment of the right middle lobe. Final diagnosis: Pulmonary neuroendocrine tumor (S100: positive; synaptophysin: negative; chromogranin: negative).

artifacts to increase the rate of detection of retrocardiac opacities by the radiologist.<sup>22</sup>

## Conclusion

A wide range of pathologies ranging from congenital anomalies like esophageal duplication cyst and bronchogenic cyst to rare tumors like pulmonary neuroendocrine tumor and cardiac papillary fibroelastoma were diagnosed merely by incidental detection and imaging workup of retrocardiac opacities in the chest radiograph. Thus, retrocardiac shadows must be carefully looked for in all chest radiographs. If detected, they must be promptly evaluated with other imaging modalities and, if required, histopathological analysis to confirm the diagnosis.

### Note

The manuscript was presented as a poster at several conferences. First, it was showcased at the IRIA State Conference, held on November 26-27, 2022, in Kollam, Kerala, India. Subsequently, it was presented at the IRIA National Conference, which took place from February 2 to 5, 2023, in Amritsar, India. Lastly, the manuscript was featured at the European Congress of Radiology, held in Vienna, Austria, from March 1 to 5, 2023.

### Funding

None.

### Conflict of Interest

None declared.

### Acknowledgments

We express our gratitude to the staff of the Department of Radiology at Kerala Institute of Medical Sciences, Thiruvananthapuram, for their valuable support.

### References

- 1 Nemeč SS. Differential diagnosis of retrocardiac shadows. *Radiology* 1948;50(02):174–183
- 2 Holmes GW. Radiographic findings in pericarditis with effusion. *AJR Am J Roentgenol* 1920;7:7–15
- 3 Freedman E, Higley CS, Hauser H. Developmental and life cycles of thoracic aortic aneurysms. *AJR Am J Roentgenol* 1939;39:720–726
- 4 Riger LG. The density of the central shadow in the diagnosis of intrathoracic lesions. *Radiology* 1939;32:316–324
- 5 Ladd WE, Scott HW. Esophageal duplications or mediastinal cysts of enteric origin. *Surgery* 1944;16:815–835
- 6 McAdams HP, Kirejczyk WM, Rosado-de-Christenson ML, Matsumoto S. Bronchogenic cyst: imaging features with clinical and histopathologic correlation. *Radiology* 2000;217(02):441–446
- 7 Jeung MY, Gasser B, Gangi A, et al. Imaging of cystic masses of the mediastinum. *Radiographics* 2002;22(suppl\_1):S79–S93

- 8 Chandler FA, Norcross JR. Sympathicoblastoma. *JAMA* 1940; 114:112–117
- 9 Spiridakis KG, Flamourakis ME, Gkionis IG, et al. Right-sided strangulating diaphragmatic hernia in an adult without history of trauma: a case report. *J Med Case Reports* 2021;15(01):372
- 10 Torfs CP, Curry CJ, Bateson TF, Honoré LH. A population-based study of congenital diaphragmatic hernia. *Teratology* 1992;46(06):555–565
- 11 Scott RL, Felker R, Winer-Muram H, Pinstein ML. The differential retrocardiac air-fluid level: a sign of intrathoracic gastric volvulus. *Can Assoc Radiol J* 1986;37(02):119–121
- 12 Kent EM, Blades B, Valle AR, Graham EA. Intrathoracic neurogenic tumors. *J Thorac Surg* 1944;13:116–161
- 13 Naffziger HC, Brown HA. Hourglass tumors of the spine. *Arch Neurol Psychiatry* 1933;29:561–584
- 14 Machiori E, Barreto MM, Hochegger B, Zanetti G. Extramedullary haematopoiesis: an uncommon posterior mediastinal mass. *S Afr J Rad* 2013;17(03):114–115
- 15 Nyman R, von Sinner W, Mygind T, Kagevi I. Paraesophageal varices presenting as a retrocardiac mediastinal mass. A case report. *Acta Radiol* 1994;35(03):255–257
- 16 Basheda SG, O'Donovan P, Golish JA. Giant esophageal varices. An unusual cause of a posterior mediastinal mass. *Chest* 1993;103(04):1284–1285
- 17 Wang YW, Lin WT. A retrocardiac opacity in a cirrhotic patient: esophageal varices. *Int J Clinical Medical Images* 2015:2376–0249
- 18 Pavlov A, Barnes S. A case of a retrocardiac mass. *IMAJ* 2018; 20:60–61
- 19 Higgins CB, Reinke RT, Jones NE, Broderick T. Left atrial dimension on the frontal thoracic radiograph: a method for assessing left atrial enlargement. *AJR Am J Roentgenol* 1978;130(02): 251–255
- 20 Devanabanda AR, Lee LS. Papillary Fibroelastoma. Treasure Island, FL: StatPearls Publishing; 2022
- 21 Queiroz RM, Santana DBF, Natri Filho R, Landell GAM, Félix PR, Valentin MVN. Endobronchial carcinoid tumor: radiological findings of a clinical case. *Rev Assoc Med Bras* 2018;64(01): 15–18
- 22 Williams MB, Krupinski EA, Strauss KJ, et al. Digital radiography image quality: image acquisition. *J Am Coll Radiol* 2007;4(06): 371–388